Chapter VI

CHAPTER VI

STABILITY ANALYSIS OF HYDROMAGNETIC INVISCID STRATIFIED PARALLEL LINEAR SHEAR FLOW

6.1 Introduction

The linear stability of stratified shear flow of an inviscid, incompressible fluid has been broadly analysed by many authors. The classical method for obtaining stability criteria from the linearized equations for an inviscid incompressible fluid in a plane parallel flow is normal-mode technique, which leads to the Rayleigh stability equation Drazin and Reid (1981), Drazin and Howard (1966)). The normal-mode stability analysis of plane parallel flows of an inviscid, incompressible stratified fluid has been analyzed by Taylor (1931) and Goldstein (1931).

Drazin (1960) examined the stability of parallel flow for small magnetic Reynolds numbers. Kent (1966, 1968) studied about the instability against small oscillations of symmetric laminar flow of an inviscid, incompressible perfectly conducting magnetofluid, in the presence of symmetric magnetic field parallel to the flow. Agarwal and Agarwal (1969) analyzed the stability of non-dissipative heterogeneous shear flow in the presence of uniform magnetic field in the streaming direction.

Kochar and Jain (1979) investigated the hydromagnetic stability of stratified shear flows and obtained a semi-ellipse region for unstable modes in the complex plane. Rathy and Harikishan (1981) discussed the stability of the flow of an inviscid, incompressible fluid of variable density between two parallel plates in the presence of magnetic field. Small perturbations of parallel shear flow in an inviscid, incompressible stably stratified fluid are studied by Collyer (1970).

The Kuo's (1949) eigen value problem governs the normal mode stability of barotropic zonal flows of an inviscid, incompressible fluid on a β - plane. Barston (1991) introduced a new method in the linear stability analysis of plane parallel flows of inviscid, incompressible homogeneous fluid. Stability of stratified shear flows in channels with variable cross section is studied in detail by Reddy and Subbiah (2015). Linear stability of inviscid, parallel and stably stratified shear flow under the

assumption of smooth strictly monotonic profiles of shear flow and density is analyzed by Hirota and Morrison (2016).

Keeping in mind the importance of Newtonian fluids in technology, industries, chemical engineering and owing to the importance of magnetic field in geophysics, astrophysics etc., we are motivated to study the linear stability of stratified shear fluid in the presence of uniform magnetic field in the present chapter. The work of Padmini and Subbiah (1995) is extended to study the effect of uniform magnetic field. The stability of stratified flow of an inviscid, incompressible fluid confined between two rigid planes at $z = \pm$L under the influence of uniform magnetic field is considered. The analysis is restricted to linear velocity profile with long wavelength approximations.

6.2 Formulation of the problem

Consider an electrically conducting stratified inviscid Boussinesq fluid flowing between two horizontal plates. A uniform magnetic field is applied. We use Cartesian coordinates *(x, y, z)* taking the mid-point between two parallel plates as origin. The plates are considered at a distance *2L* apart. The fluid is acted on by gravity force *g(0, 0, -g).* Under the above mentioned assumptions the schematic representation of the problem is given in Figure 6.1.

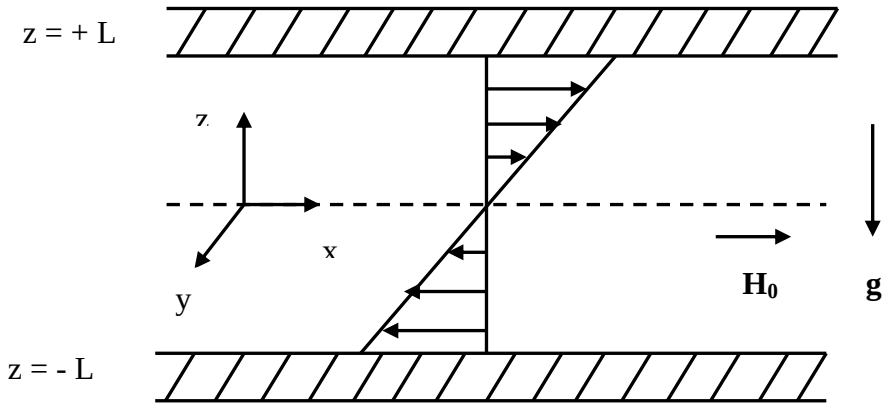

Figure 6.1: Schematic representation of the problem

With the Boussinesq's approximation, the governing equations for the motion of an inviscid, incompressible, stratified shear fluid confined between two horizontal infinite rigid planes under horizontal magnetic field are

$$\nabla.\vec{q} = 0 \tag{6.1}$$

$$\frac{\partial\vec{q}}{\partial t} + (\vec{q}.\nabla)\vec{q} = \frac{-\nabla p}{\rho_0} - \frac{\rho g\hat{z}}{\rho_0} + \mu_m(\nabla\times\vec{H})\times\vec{H} \tag{6.2}$$

$$\frac{\partial \rho}{\partial t} + (\vec{q}.\nabla)\rho = 0 \quad (6.3)$$

$$\frac{\partial \vec{H}}{\partial t} = \eta \nabla^2 \vec{H} + \nabla \times (\vec{q} \times \vec{H}) \quad (6.4)$$

$$\nabla.\vec{H} = 0 \quad (6.5)$$

where $\vec{q}$, ρ, p, g, η, μ_m and $\vec{H}$ denote the velocity, density, pressure, acceleration due to gravity, resistivity, magnetic permeability and the magnetic field respectively.

If the fluid is confined between two horizontal rigid planes at z = ±L, the boundary conditions are

$$\vec{q} = 0 \qquad \text{at } z = \pm L \quad (6.6)$$

The equilibrium state is given by

$$-\frac{\partial p_e}{\partial z} - \rho_e g = 0 \quad (6.7)$$

The dimensionless forms have been rendered for the quantities with respect to the characteristic length (L) and the characteristic velocity (U_0) as the following:

$$t = \frac{Lt^*}{U_0},\ p = \rho_0 U_0^2 p^*,\ \rho = \frac{\rho_0 U_0^2 N_0^2}{Lg}\rho^*,\ \vec{H} = H_0 \vec{H}^*$$

and $(x,y,z) = L(x^*,y^*,z^*)$ (6.8)

where $N^2 = -\frac{g}{\rho_0}\left(\frac{d\rho}{dz}\right)$ is the Brunt-Vaisala frequency which is assumed to be positive for static stability and N_0^2 is a typical value of Brunt-Vaisala frequency in the flow domain. Substitute the above dimensionless quantities in the governing equations, equations (6.1) - (6.5) reduce to (on removing asterisks)

$$\nabla.\vec{q} = 0 \quad (6.9)$$

$$\frac{\partial \vec{q}}{\partial t} + (\vec{q}.\nabla)\vec{q} = -\nabla p - Ri\, g\hat{k} + S(\nabla \times \vec{H}) \times \vec{H} \quad (6.10)$$

$$\frac{\partial \rho}{\partial t} + (\vec{q}.\nabla)\rho = 0 \quad (6.11)$$

$$\frac{\partial \vec{H}}{\partial t} = \frac{1}{Rm}\nabla^2 \vec{H} + \nabla \times (\vec{q} \times \vec{H}) \quad (6.12)$$

$$\nabla.\vec{H} = 0 \quad (6.13)$$

where $S = \frac{\mu_m H_0^2}{\rho U_0^2}$, Magnetic Pressure Number

$Rm = \frac{LU_0}{\eta}$, Magnetic Reynolds Number

$Ri = \frac{g\beta L^2}{\rho_0 U_0^2}$, Richardson Number

The boundary condition in non-dimensional form is

$$\vec{q} = 0 \qquad \text{on } z = \pm 1 \quad (6.14)$$

Decomposing the flow into basic state and disturbed as $(U(z)+u, v, w)$, $\rho_e(z)+\rho$, $p_e(z)+p$ and $(H_0+h_x,\ h_y,\ h_z)$, the basic state $U(z), \rho_e, p_e, H_0$ are governed by the equations above.

The linearized perturbation equations for infinitesimal normal modes of the form $f(z)e^{ik(x+ly-\sigma t)}$, ($k$, l and σ are the horizontal, transverse wave number and the complex wave velocity respectively) are obtained as

$$
\begin{aligned}
ik(u+lv)+\frac{\partial w}{\partial z} &= 0\\
ik(U-\sigma)u + w.\frac{\partial U}{\partial z} &= -ik\left(p + H_0 S\left(h_y - lh_x\right)\right)\\
ik(U-\sigma)v &= -ik\left(p - H_0 S\left(h_y - lh_x\right)\right)\\
ik(U-\sigma)w &= -\frac{\partial p}{\partial z} - Ri\,\rho\\
&\quad + H_0 S\left(ik(1+l)h_z - \frac{\partial h_y}{\partial z} - \frac{\partial h_x}{\partial z}\right)\\
ik(U-\sigma)\rho - \frac{N^2}{N_0^2}w &= 0\\
ik\left(h_x + lh_y\right) + \frac{\partial h_z}{\partial z} &= 0\\
\left(-ik\sigma - \frac{1}{Rm}\left(-k^2(1+l^2) + \frac{\partial^2}{\partial y^2}\right)\right)h_x &= ikl\left(H_0 u + Uh_y - H_0 v\right)\\
&\quad - H_0\frac{\partial w}{\partial z} + \frac{\partial}{\partial z}(Uh_z)\\
\left(-ik\sigma - \frac{1}{Rm}\left(-k^2(1+l^2) + \frac{\partial^2}{\partial y^2}\right)\right)h_y &= -ik\left(H_0 u + Uh_y - H_0 v\right) - H_0\frac{\partial w}{\partial z}\\
\left(-ik\sigma - \frac{1}{Rm}\left(-k^2(1+l^2) + \frac{\partial^2}{\partial y^2}\right)\right)h_z &= ik\left((1+l)H_0 w - Uh_z\right) \qquad (6.15)
\end{aligned}
$$

The associated boundary conditions are

$$u = v = w = 0 \qquad \text{on} \quad z = \pm 1 \qquad (6.16)$$

6.3 Eigen values and eigen functions for long waves

Here, we consider the analysis for long wave approximation (i.e) k is assumed to be small and the flow is assumed to be bounded between two plates $z = \pm 1$. In order to get closed form solutions, we consider the linear velocity profile as the basic flow $U(z) = z$.

Hence equation (6.15) reduces to the form

$$
\begin{aligned}
ik(u+lv)+\frac{\partial w}{\partial z} &= 0\\
ik(-\sigma+z)u + w &= -ik\left(p + H_0 S\left(h_y - lh_x\right)\right)
\end{aligned}
$$

$$
\begin{aligned}
ik(-\sigma + z)v &= -ik\left(p - H_0 S\left(h_y - l h_x\right)\right) \\
ik(-\sigma + z)w &= -\frac{\partial p}{\partial z} - Ri\,\rho + H_0 S\left(ik(1+l)h_z - \frac{\partial h_y}{\partial z} - \frac{\partial h_x}{\partial z}\right) \\
ik(-\sigma + z)\rho - \frac{N^2}{N_0^2} w &= 0 \\
ik\left(h_x + l h_y\right) + \frac{\partial h_z}{\partial z} &= 0 \\
\left(-ik\sigma - \frac{1}{Rm}\left(-k^2(1+l^2) + \frac{\partial^2}{\partial y^2}\right)\right) h_x &= ikl\left(H_0 u + z h_y - H_0 v\right) \\
&\quad - H_0 \frac{\partial w}{\partial z} + \frac{\partial}{\partial z}(z h_z) \\
\left(-ik\sigma - \frac{1}{Rm}\left(-k^2(1+l^2) + \frac{\partial^2}{\partial y^2}\right)\right) h_y &= -ik\left(H_0 u + z h_y - H_0 v\right) - H_0 \frac{\partial w}{\partial z} \\
\left(-ik\sigma - \frac{1}{Rm}\left(-k^2(1+l^2) + \frac{\partial^2}{\partial y^2}\right)\right) h_z &= ik\left((1+l)H_0 w - z h_z\right) \qquad (6.17)
\end{aligned}
$$

We assume the series expansions with respect to the wave number *k* in the form

$$f = f_0 + k f_1 + k^2 f_2 + \cdots \qquad (6.18)$$

where f represents any one of the disturbances $u,\ v,\ w,\ \sigma,\ \rho,\ h_x,\ h_y$ or h_z

Substituting equation (6.18) into equation (6.17) and equating the coefficients of same degree terms and neglecting k^2 we get the following set of differential equations:

Zeroth order equations:

$$
\begin{aligned}
iu_0 + ilv_0 + \frac{\partial w_0}{\partial z} &= 0 \\
iT(z)u_0 + w_0 &= -ip_0 \\
iT(z)v_0 &= -ilp_0 \\
-\frac{\partial p_0}{\partial z} - Ri\,\rho_0 &= 0 \\
iT(z)\rho_0 - \frac{N^2}{N_0^2} w_0 &= 0 \qquad (6.19) \\
ih_{x0} + ilh_{y0} + \frac{\partial h_{z0}}{\partial z} &= 0 \\
-\frac{1}{Rm}\left(\frac{\partial^2 h_{x0}}{\partial z^2}\right) &= i(1+l)H_0 u_0 \\
-\frac{1}{Rm}\left(\frac{\partial^2 h_{y0}}{\partial z^2}\right) &= i(1+l)H_0 v_0 \\
-\frac{1}{Rm}\left(\frac{\partial^2 h_{z0}}{\partial z^2}\right) &= i(1+l)H_0 w_0 \qquad (6.20)
\end{aligned}
$$

where $T(z) = z - \sigma_0$

First order equations:

$$
\begin{aligned}
iu_1 + ilv_1 + \frac{\partial w_1}{\partial z} &= 0 \\
iT(z)u_1 + w_1 - i\sigma_1 u_0 &= -ip_1 - iH_0 S\left(h_{y0} - lh_{x0}\right) \\
iT(z)v_1 - i\sigma_1 v_0 &= -ilp_1 + iH_0 S\left(h_{y0} - lh_{x0}\right) \\
\frac{\partial p_1}{\partial z} + Ri\,\rho_1 &= -H_0 S\left(\frac{\partial h_{x0}}{\partial z} + \frac{\partial h_{y0}}{\partial z}\right) \\
iT(z)w_1 - i\sigma_1 w_0 &= -ilp_1 - Slh_{x0}(1+y) \\
iT(z)\rho_1 - i\sigma_1\rho_0 - \frac{N^2}{N_0^2}w_1 &= 0 \qquad (6.21)
\end{aligned}
$$

$$
\begin{aligned}
ih_{x1} + ilh_{y1} + \frac{\partial h_{z1}}{\partial z} &= 0 \\
-\frac{1}{Rm}\left(\frac{\partial^2 h_{x1}}{\partial z^2}\right) &= i(1+l)u_1 H_0 - iT(z)h_{x0} + h_{z0} \\
-\frac{1}{Rm}\left(\frac{\partial^2 h_{y1}}{\partial z^2}\right) &= i(1+l)v_1 H_0 - iT(z)h_{y0} \\
-\frac{1}{Rm}\left(\frac{\partial^2 h_{z1}}{\partial z^2}\right) &= i(1+l)w_1 H_0 - iT(z)h_{z0} \qquad (6.22)
\end{aligned}
$$

The boundary conditions (6.16) reduce to

$$u_0 = u_1 = 0, \quad v_0 = v_1 = 0, \; w_0 = w_1 = 0 \qquad (6.23)$$

By simplifying equation (6.19) in terms of w_0, we get

$$T(z)^2 \frac{\partial^2 w_0}{\partial z^2} + \frac{Ri\,N^2}{{N_0}^2}(1+l^2)w_0 = 0 \qquad (6.24)$$

The solution of equation (6.24) is given by

$$
w_0 = \begin{cases} A\,T(z)^{m_1} + B\,T(z)^{m_2}, & \lambda > 0 \\ T(z)^{\frac{1}{2}}(C + D\,log\,(T(z)), & \lambda = 0 \\ T(z)^{\frac{1}{2}}\left(Ecos\left(klog(T(z))\right) + Fsin\left(klog(T(z))\right)\right), & \lambda < 0 \end{cases}
$$

where $m_{1,2} = \frac{1 \pm \sqrt{\lambda}}{2}$, $\lambda = 1 - 4\,Ri\,\frac{N^2}{N_0^2}(1+l^2)$, $k = \frac{\sqrt{-\lambda}}{2}$, *A*, *B*, *C*, *D*, *E* and *F* are arbitrary constants.

By applying the boundary conditions that the velocity should vanish at the boundaries (i.e) $w_0 = 0 \;\; at\; z = \pm 1$, we obtain the value of σ_0 as

$$
\sigma_0 = \begin{cases} \dfrac{1+e^{\frac{2n\pi i}{m_1 - m_2}}}{1-e^{\frac{2n\pi i}{m_1 - m_2}}}, & \lambda \geq 0 \\ \dfrac{1+e^{\frac{n\pi}{k}}}{1-e^{\frac{n\pi}{k}}}, & \lambda < 0 \end{cases} \qquad (6.25)
$$

The solution of equations (6.19) and (6.20) can be obtained as

$$u_0 = \begin{cases} D_7 T(z)^{m_1-1} + C_8 T(z)^{m_2-1}, & \lambda \geq 0 \\ \frac{T(z)^{\frac{1}{2}}}{i}\left(cos\left(klog\left(T(z)\right)\right)\left(\frac{\frac{E}{2}-kF}{1+l^2} - E\right) + sin\left(klog(T(z))\right)\left(\frac{kE+\frac{F}{2}}{1+l^2} - F\right)\right), & \lambda < 0 \end{cases}$$

$$v_0 = \begin{cases} D_5 T(z)^{m_1-1} + D_6 T(z)^{m_2-1}, & \lambda \geq 0 \\ \frac{-lT(z)^{-\frac{1}{2}}}{i(1+l^2)}\left(cos\left(klog\left(T(z)\right)\right)\left(kF - \frac{E}{2}\right) + sin\left(klog(T(z))\right)\left(\frac{kE+\frac{F}{2}}{1+l^2} - F\right)\right), & \lambda < 0 \end{cases}$$

$$w_0 = \begin{cases} T(z)^{m_1} + BT(z)^{m_2}, & \lambda \geq 0 \\ T(z)^{\frac{1}{2}}\left(cos\left(klog\left(T(z)\right)\right) + sin\left(klog(T(z))\right)\right), & \lambda < 0 \end{cases}$$

$$\rho_0 = \begin{cases} D_1 T(z)^{m_1-1} + D_2 T(z)^{m_2-1}, & \lambda \geq 0 \\ \frac{N^2 T(z)^{-\frac{1}{2}}}{iN_0^2}\left(cos\left(klog\left(T(z)\right)\right) + Fsin\left(klog(T(z))\right)\right), & \lambda < 0 \end{cases}$$

$$p_0 = \begin{cases} D_3 T(z)^{m_1} + D_4 T(z)^{m_2}, & \lambda \geq 0 \\ \frac{T(z)^{\frac{1}{2}}}{i(1+l^2)}\left(cos\left(klog\left(T(z)\right)\right)\left(kF - \frac{1}{2}\right) + sin\left(klog(T(z))\right)\left(-k - \frac{F}{2}\right)\right), & \lambda < 0 \end{cases}$$

$$h_{x0} = Rm \begin{cases} D_{11}\, T(z)^{m_1+1} + D_{12}\, T(z)^{m_2+1}, & \lambda \geq 0 \\ T(z)^{\frac{3}{2}}\left(D_{44} cos\left(klog\left(T(z)\right)\right) + C_{45}\, sin\left(klog(T(z))\right)\right), & \lambda < 0 \end{cases}$$

$$h_{y0} = Rm \begin{cases} D_{13}\, T(z)^{m_1+1} + D_{14}\, T(z)^{m_2+1}, & \lambda \geq 0 \\ T(z)^{\frac{3}{2}}\left(C_{42}\, cos\left(klog\left(T(z)\right)\right) + C_{43} sin\left(klog\left(T(z)\right)\right)\right), & \lambda < 0 \end{cases}$$

$$h_{z0} = Rm \begin{cases} D_9\, T(z)^{m_1+2} + D_{10}\, T(z)^{m_2+2}, & \lambda \geq 0 \\ T(z)^{\frac{5}{2}}\left(D_{40} cos\left(klog\left(T(z)\right)\right) + D_{41} sin\left(klog(T(z))\right)\right), & \lambda < 0 \end{cases}$$

Equation (6.21) is simplified interms of w_1 as

$$T(z)^2 \frac{\partial^2 w_1}{\partial z^2} + \frac{Ri\, N^2}{{N_0}^2}(1+l^2) w_1 = \sigma_1 \left(T(z)^2 \frac{\partial^2 w_0}{\partial z^2} - Ri\,(1+l^2)\, i\, \rho_0\right) - iH_0 S\,(1+l) T(z)\left(\frac{\partial\, h_{x0}}{\partial z} + \frac{\partial\, h_{y0}}{\partial z}\right) \quad (6.26)$$

The value of σ_1 can be obtained from the above equation by applying the boundary condition that $v_1(\pm 1) = 0$

$$\sigma_1 = \begin{cases} \frac{S\, Rm\, D_{39}}{Ri\, D_{37} - D_{38}}, & \lambda \geq 0 \\ \frac{-S\, Rm\, D_{62}}{D_{61}}, & \lambda < 0 \end{cases} \quad (6.27)$$

For the sake of brevity the constants are given in *Appendix IV*.

6.4 Results and Discussion

In this work, we have presented the numerical results concerning linear stability of an inviscid, incompressible hydromagnetic stratified shear flow by considering the basic state velocity profile as linear. To determine the effects of the

system parameters on the wave numbers, we plot the growth rate as a function of various dimensionless parameters. Figures (6.2) – (6.11) depict the growth rate as a function of wave number and Magnetic Reynolds number for various parameters when $\lambda > 0$.

Figure (6.2) shows the effect of Magnetic Reynolds number (*Rm)* on the growth rate. It shows that increase in Magnetic Reynolds number increases the growth rate with the increase in wave number thereby instability is triggered. Figure (6.3) shows the effect of Magnetic pressure number (*S*) on the growth rate. It is found that increasing magnetic pressure number leads to increase in the growth rate and have a destabilizing effect. The variation of growth rate with wave number is shown in Figure (6.4) for various values of *l*. It is seen from Figure (6.4) that increase in *l* increases the growth rate. It means that due to the increase in transverse wave number the flow becomes unstable.

In Figure (6.5) the growth rate for various n is given. It shows that, there exists infinite number of modes for the given stability problem. In Figure (6.6) we present the variation of growth rate with respect to wave number for different values of *Ri*. The result indicates that growth rate increases with *Ri* for unstable disturbances and for small Richardson number the flow becomes stable and as Richardson number increases the flow becomes unstable. Figure (6.7) depicts the dependence of the growth rate on Magnetic Reynolds number for various values of *k* when *Ri* = 0.1. From this, we conclude that with the increase in *k* the growth rate increases and leads to unstable disturbances.

The variation of growth rate with *Rm* for different values of *l* is displayed in Figure (6.8). The result indicates that increase in *l* decreases the growth rate thereby destabilizes the flow field. Figure (6.9) shows the nature of growth rate with *Rm* for various values of *Ri*. It is understood from the figure that growth rate increases with the increase in *Ri* and results in unstable disturbances. Figure (6.10) shows the growth rates of the unstable modes for various Magnetic Reynolds number (*Rm*). Figure (6.11) portrays the growth rate as a function of Brunt-Vaisala frequency. It is noticed that increasing Brunt-Vaisala frequency stabilizes the system.

Figures (6.12) – (6.20) give the idea about growth rate vs wave number, Magnetic Reynolds number and Magnetic pressure number when $\lambda < 0$**.** The growth

rate as a function of wave number is given in Figure (6.12) and Figure (6.13) for several values of *Rm*. We can see from both the figures that the disturbances are stable for small as well as large Magnetic Reynolds number. Figures (6.14) and (6.15) depict the growth rate as a function of wave number for small (S << 1) and large (S >> 1) Magnetic pressure number. It is observed from these figures that the flow becomes stable in both cases.

The growth rate is shown in Figure (6.16) as a function of wave number. It is found from the figure that the flow field is stable for smaller values of Brunt-Vaisala frequency and becomes unstable for larger Brunt-Vaisala frequency. Figure (6.17) gives the growth rate as a function of wave number for different *l*. It is seen that the fluid becomes unstable with an increase in *l*. The growth rate as a function of wave number is shown through Figures (6.18) and (6.19) for n and *Ri*. It is found from Figure (6.18) that there exists infinite number of normal modes for the given system. From Figure. (6.19), it is evident that increase in *Ri* stabilizes the fluid flow.

Figure (6.20) shows the variation of growth rate as a function of *Rm* for various *k*. It is observed that increase in *k* depreciates the growth rate thereby stabilize the system. Figure (6.21) depicts the growth rate interms of Magnetic pressure number for different *k*. It is noticed that increase in *k* declines the growth rate and therefore the system becomes stable. Figures (6.22) – (6.25) show the velocity profile for various non dimensional parameters. It is observed that the velocity profile increases with the increase in *k* and *l* when $\lambda > 0$. Velocity profile decreases with the increase in *k* and increases with the increase in *Ri* when $\lambda < 0$.

6.5 Conclusion

We have analyzed in this work the effect of magnetic field on the linear stability of an idealized stratified shear flow using series expansion method. Here we have discussed different cases and estabilized the conditions for stability. Analysis is made using normal mode approach to study the stability of fluid flow and the analysis is restricted to long wave approximation. The effects of various nondimensional numbers like Magnetic pressure number, Magnetic Reynolds number, longitudinal wave number, transverse wave number, Brunt- Vaisala frequency and Richardson number on the stability of parallel shear flow confined between the plates at $z = \pm$L is studied.

From the results obtained, it is concluded that

- Richardson number plays a significant role in the stability of parallel stratified shear flows.
- Increase in wave number increases the growth rate for varying Magnetic Pressure number and Magnetic Reynolds number when $\lambda > 0$ thereby destabilizes the flow.
- Increase in transverse wave number destabilizes the fluid flow.
- With the increase in Richardson number the flow becomes unstable ($\lambda > 0$)
- The flow becomes unstable with the increase in wave number as Magnetic Reynolds number increases.
- As Magnetic Reynolds number increases, the flow is unstable for increase in Richardson number and Magnetic Pressure number.
- As Brunt – Vaisala frequency increases, fluid flow becomes stable.
- Increase in Magnetic Reynolds number, Magnetic Pressure number and Richardson number stabilize the fluid flow with the increase in wave number when $\lambda < 0$.
- Increase in Brunt – Vaisala frequency and transverse wave number results in instability of the flow region.
- Growth rate decreases for varying wave number and thereby stabilizes the flow with the increase in Magnetic Reynolds number and Magnetic Pressure number ($\lambda < 0$).

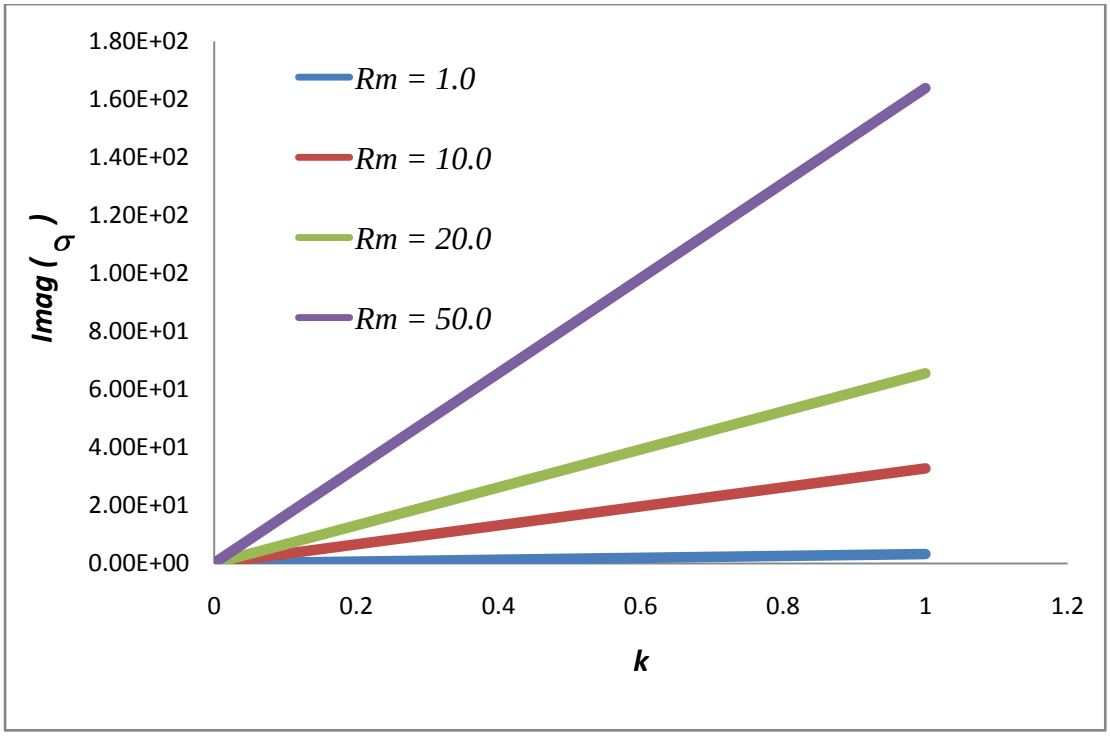

Figure 6.2: Growth rate as a function of wave number for various Rm

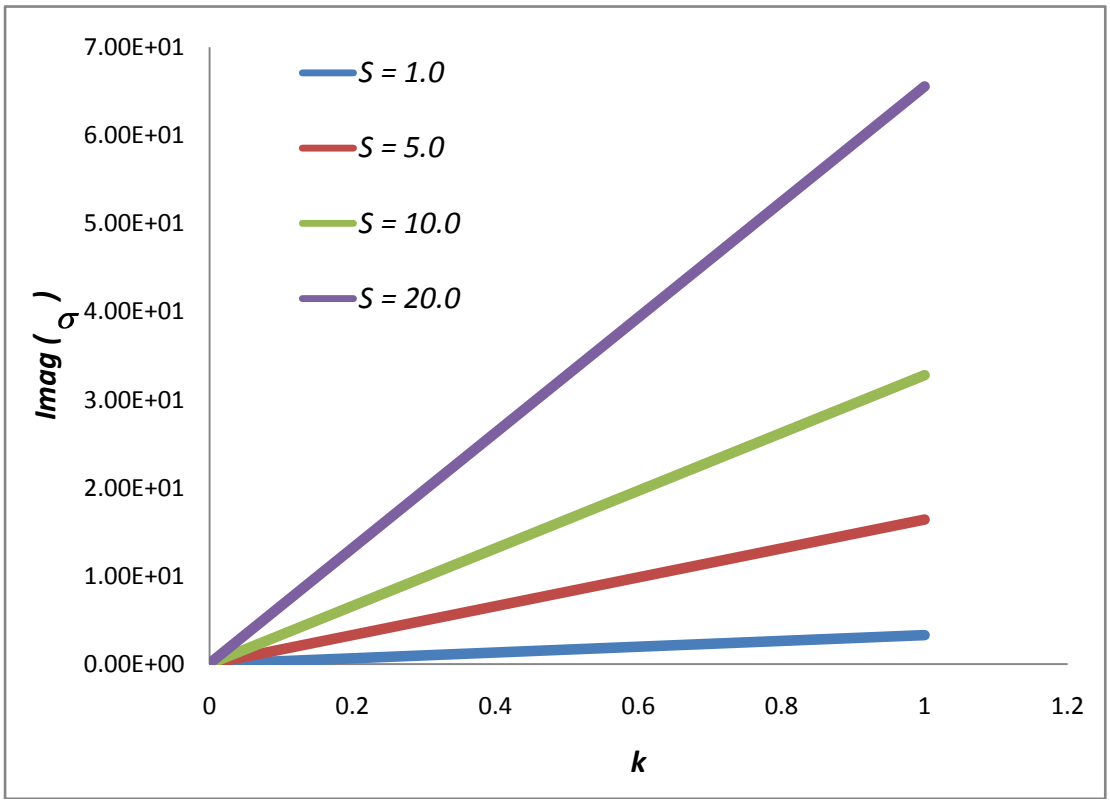

Figure 6.3: Growth rate as a function of wave number for various S

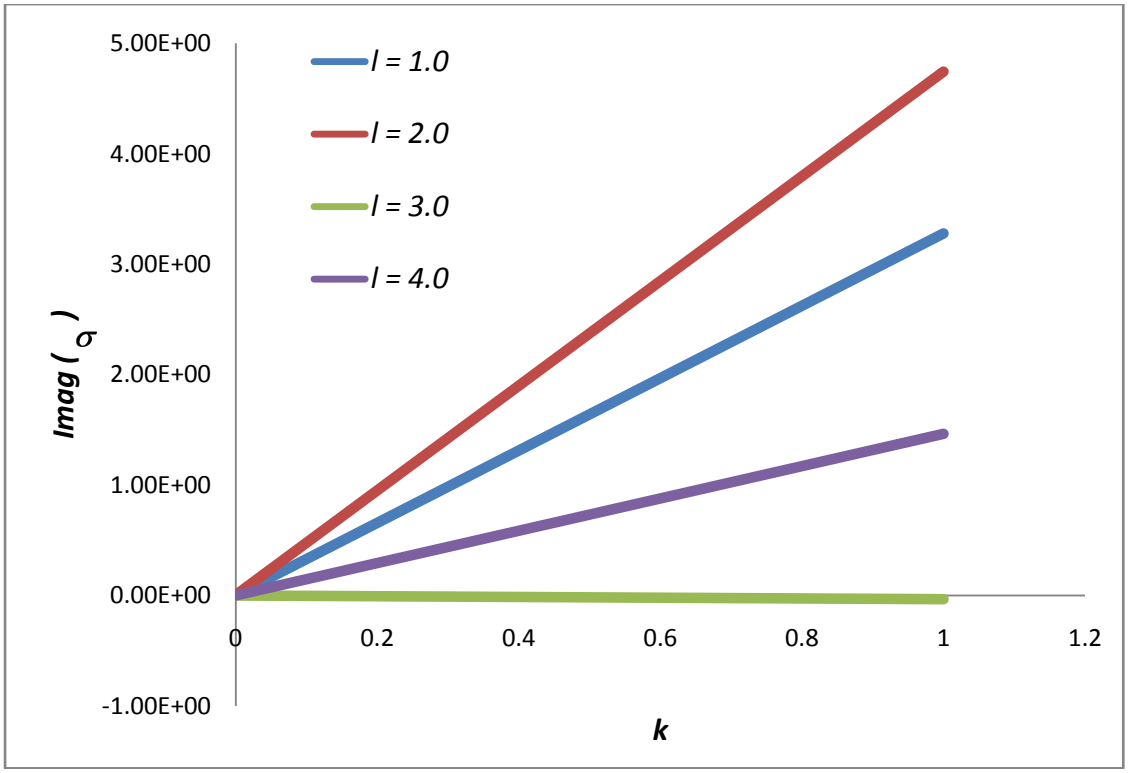

Figure 6.4: Growth rate as a function of wave number for various l

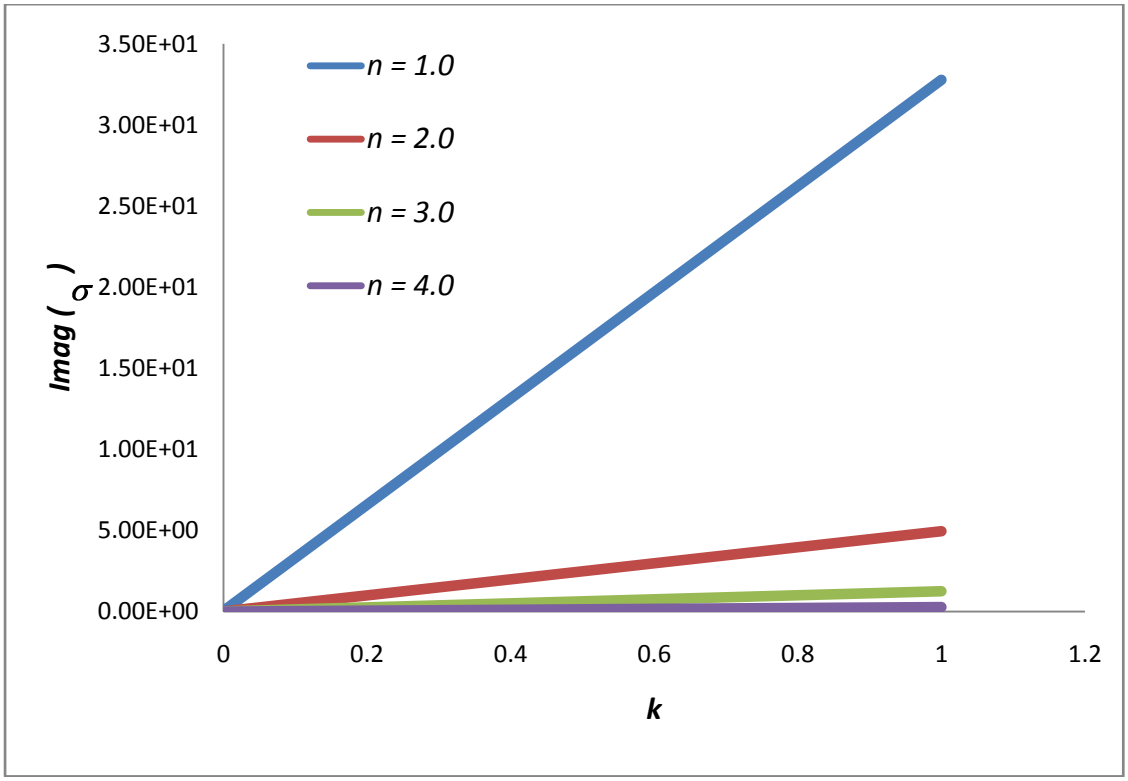

Figure 6.5: Growth rate as a function of wave number for various n

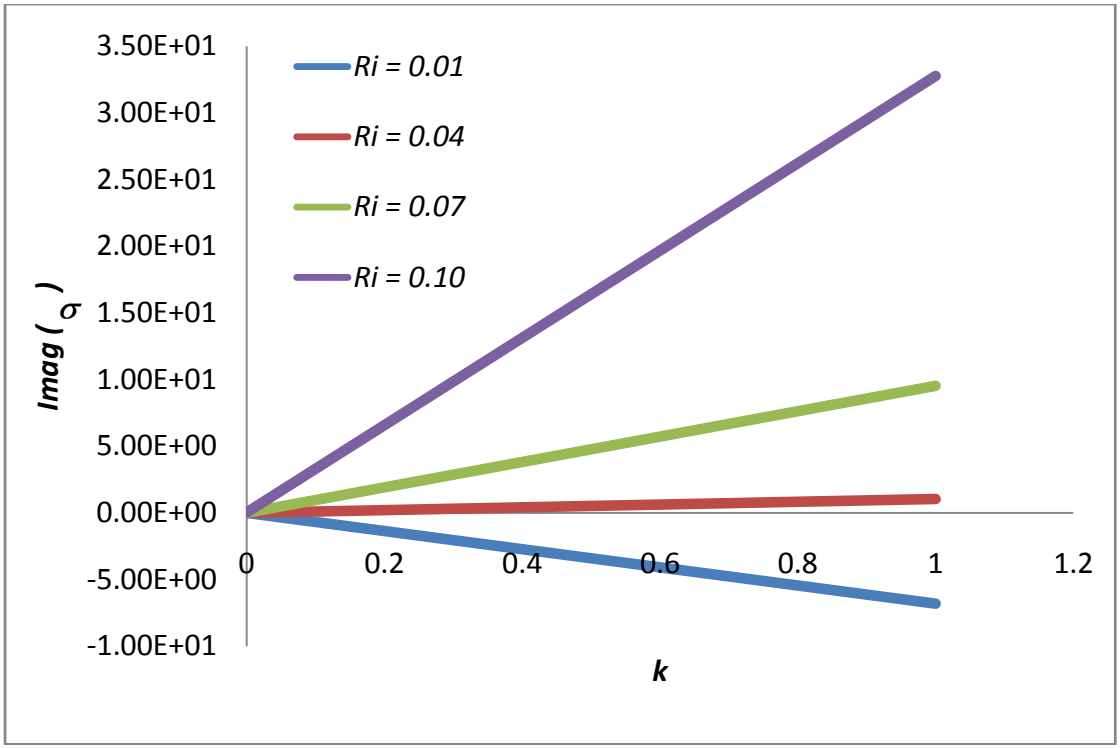

Figure 6.6: Growth rate as a function of wave number for carious Ri

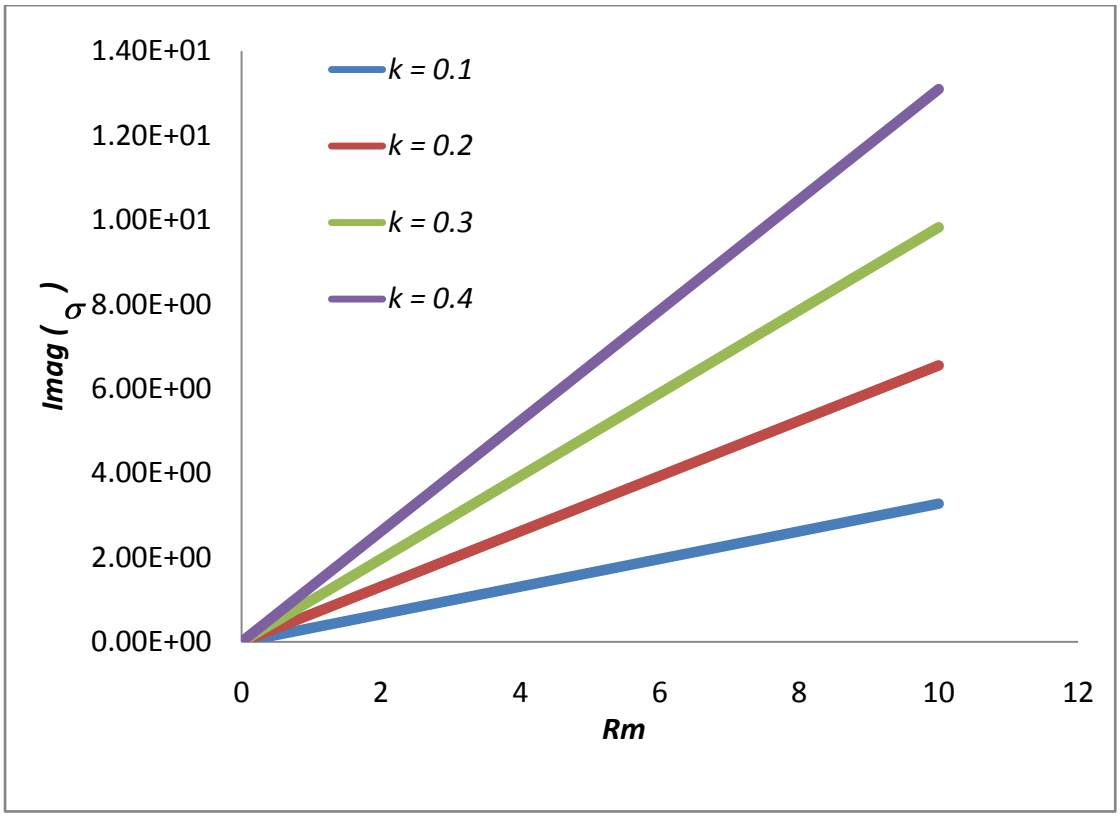

Figure 6.7: Growth rate as a function of Magnetic Reynolds number for various k

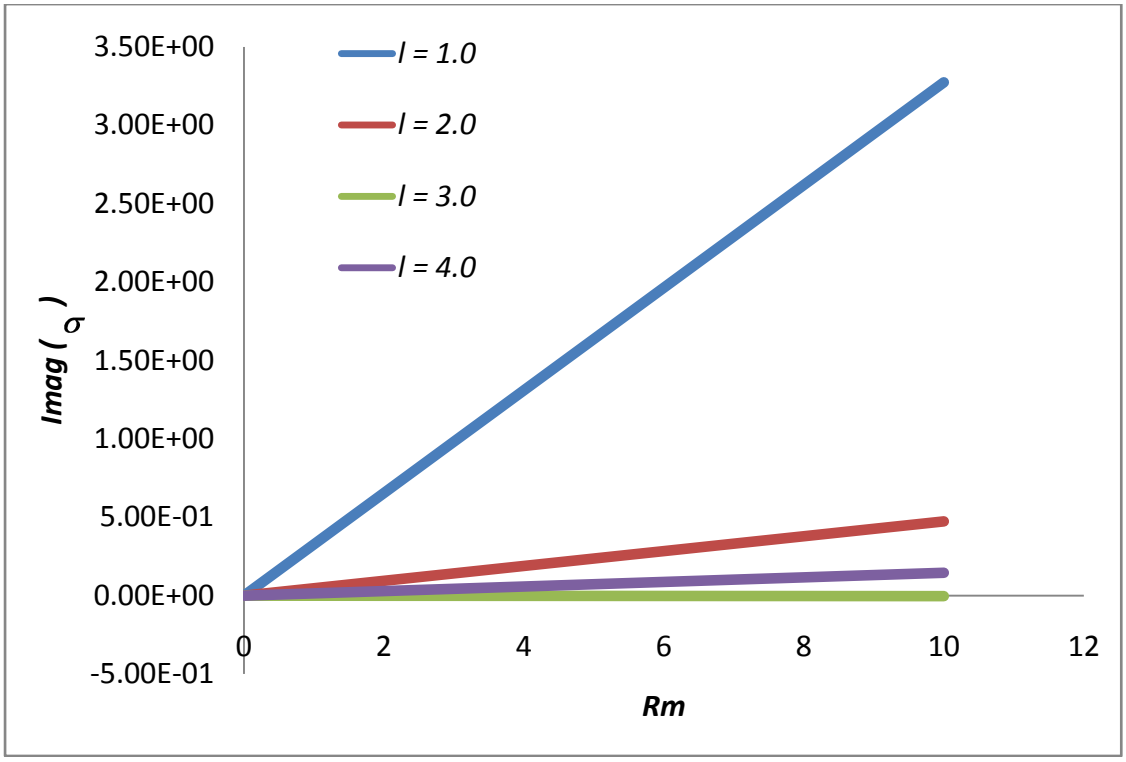

Figure 6.8: Growth rate as a function of Magnetic Reynolds number for various l

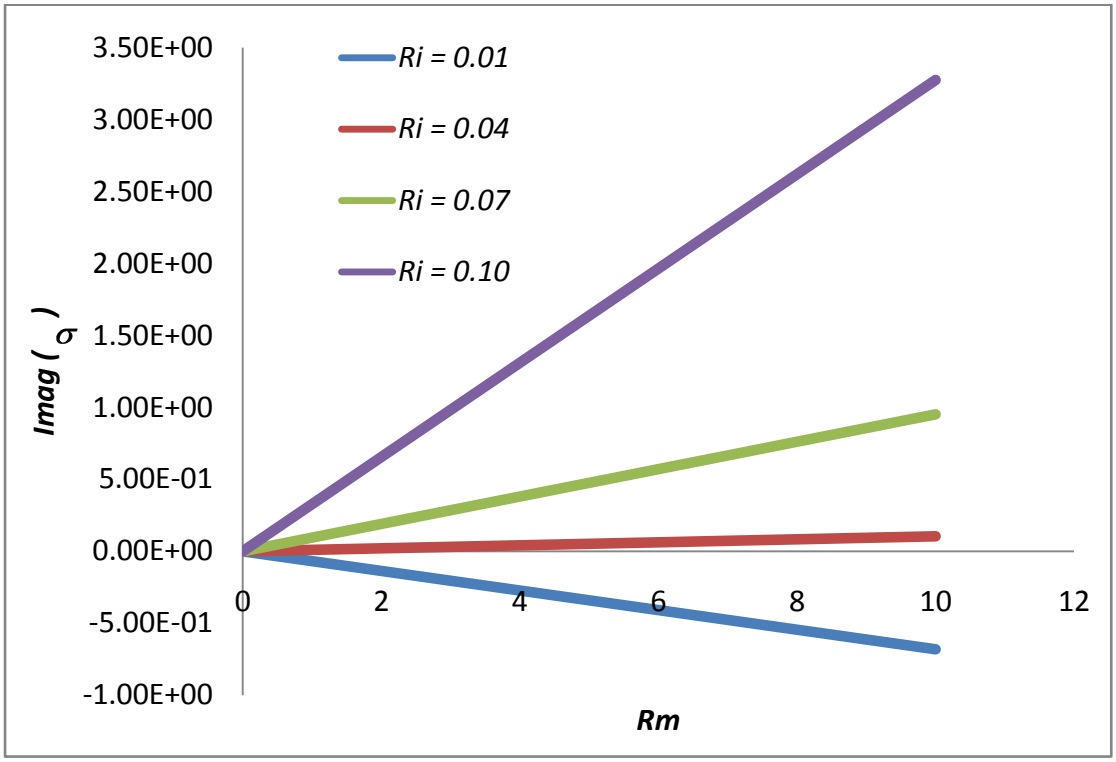

Figure 6.9: Growth rate as a function of Magnetic Reynolds number for various Ri

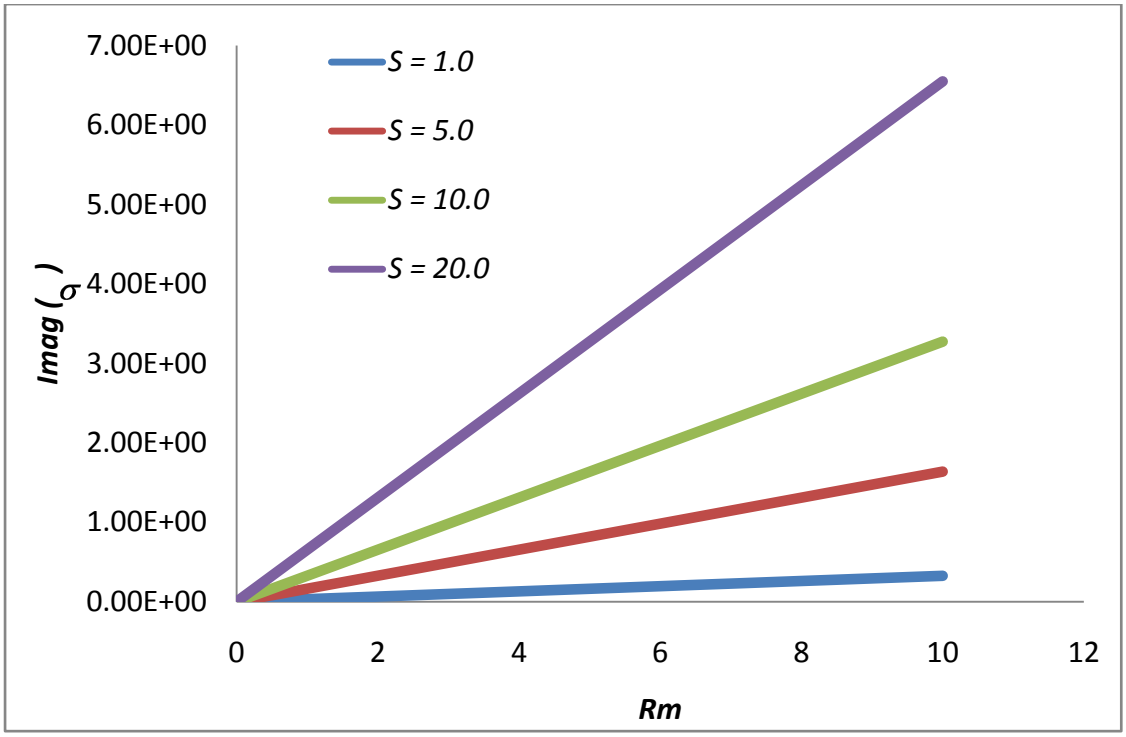

Figure 6.10: Growth rate as a function of Magnetic Reynolds number for various S

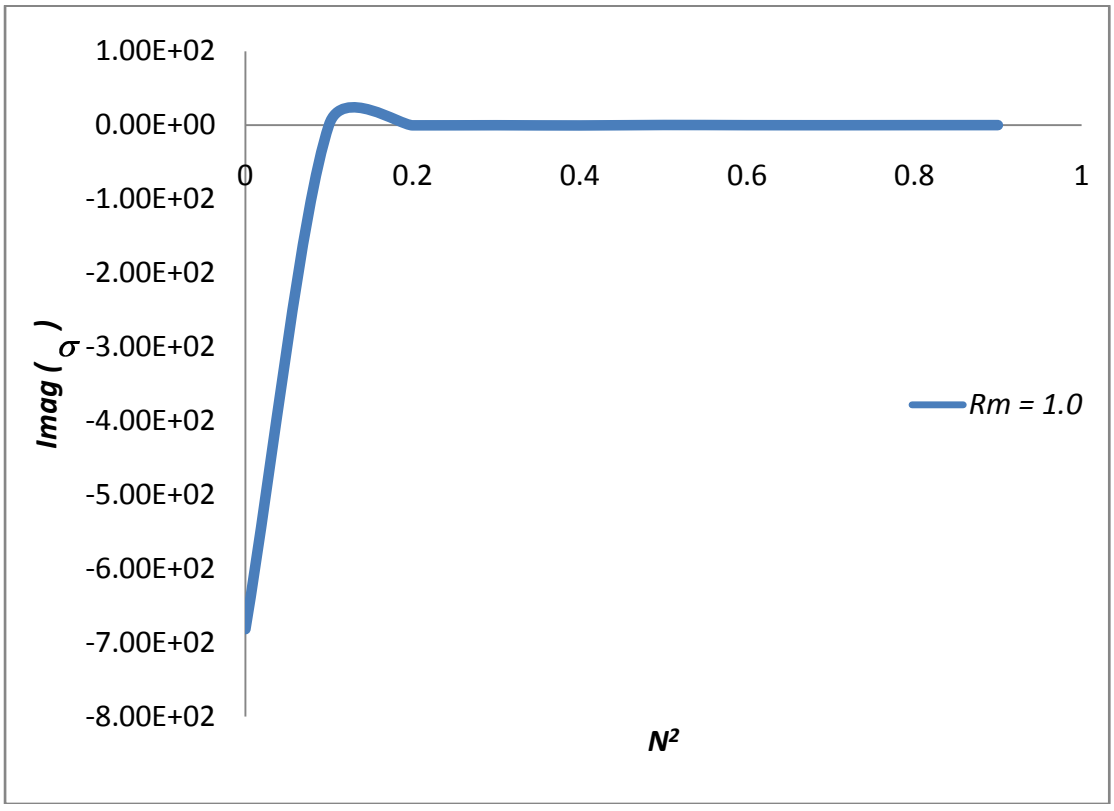

Figure 6.11: Growth rate as a function of Brunt – Vaisala frequency N^2

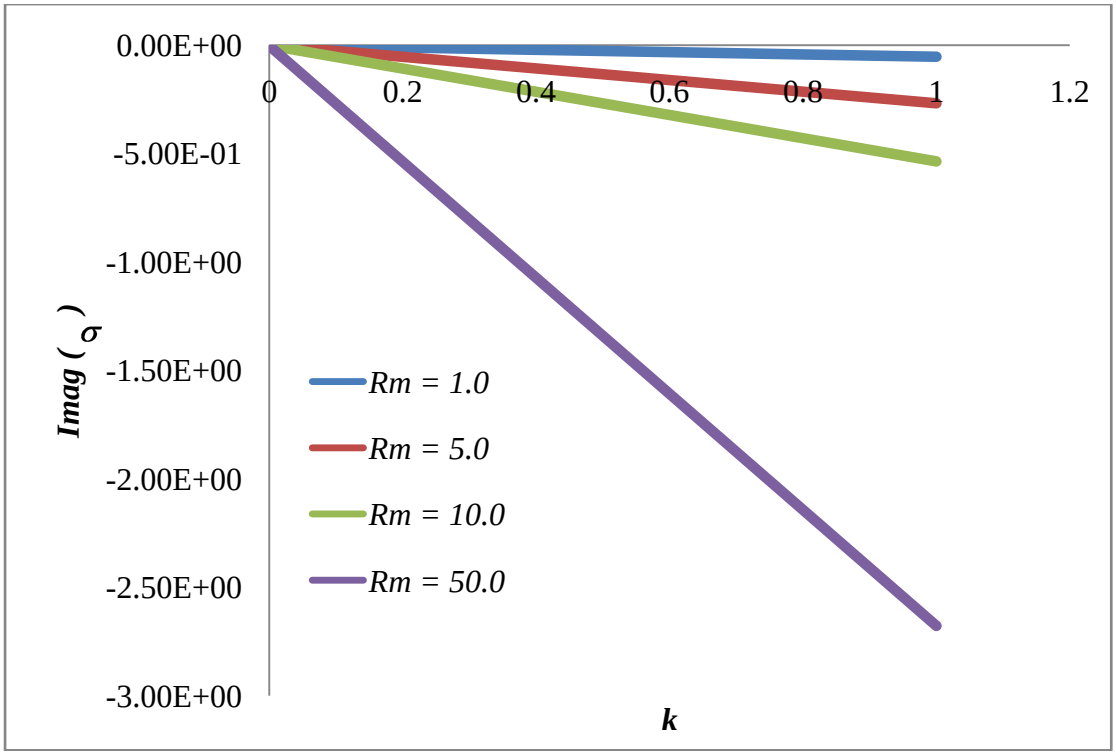

Figure 6.12: Growth rate as a function of wave number for various Rm

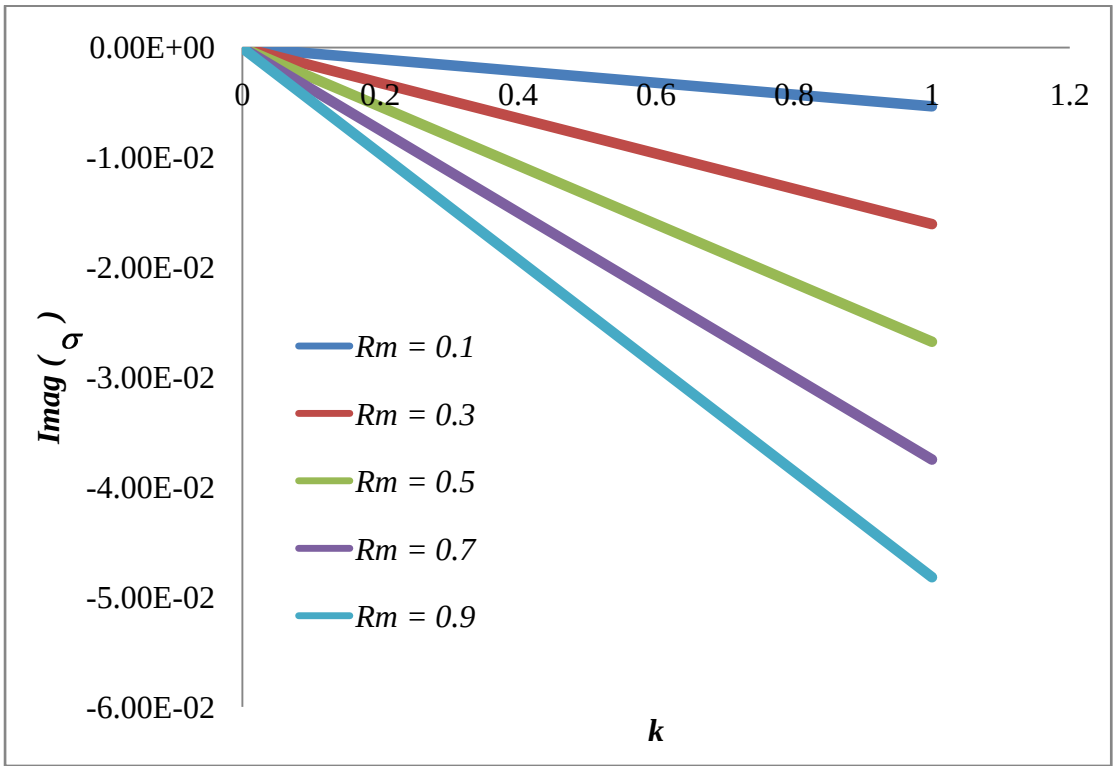

Figure 6.13: Growth rate as a function of wave number for various Rm (Rm < 1)

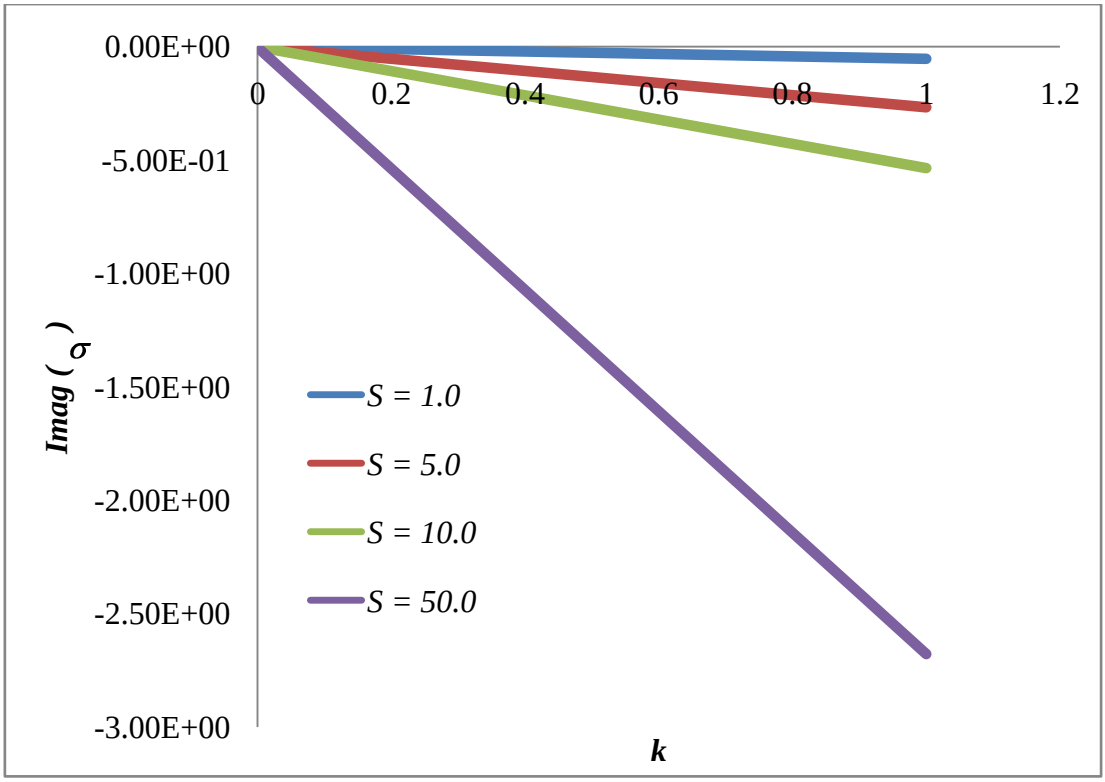

Figure 6.14: Growth rate as a function of wave number for various S

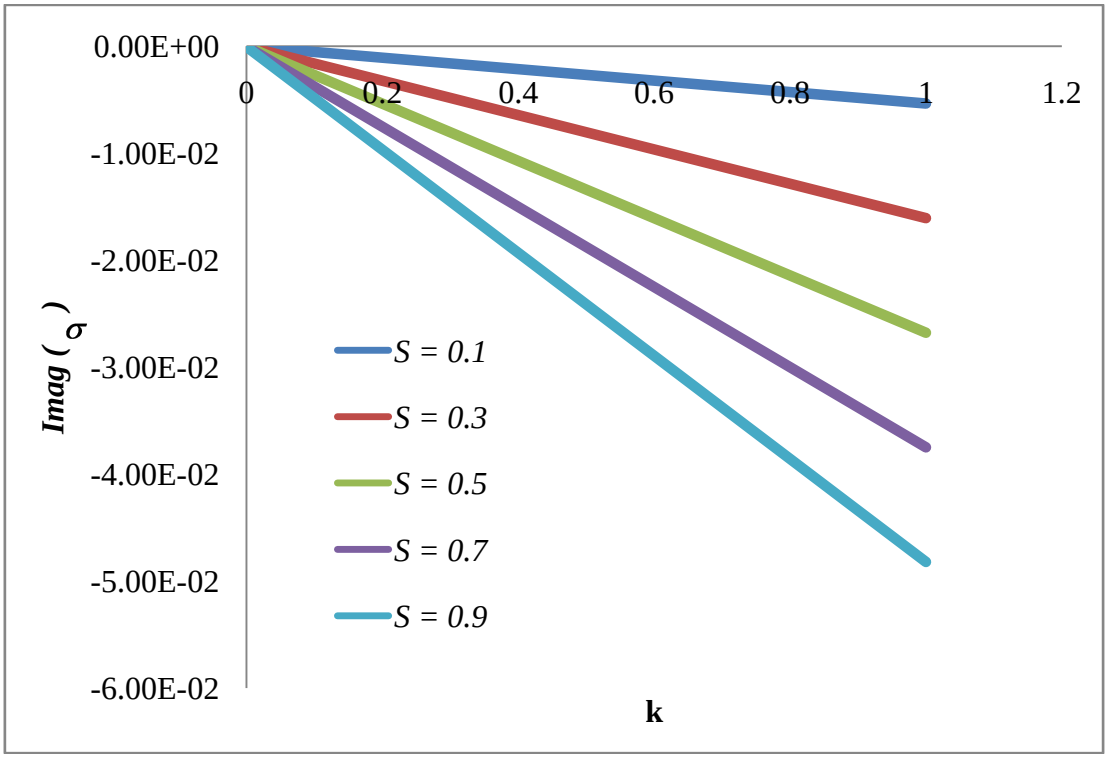

Figure 6.15: Growth rate as a function of wave number for various S (S < 1)

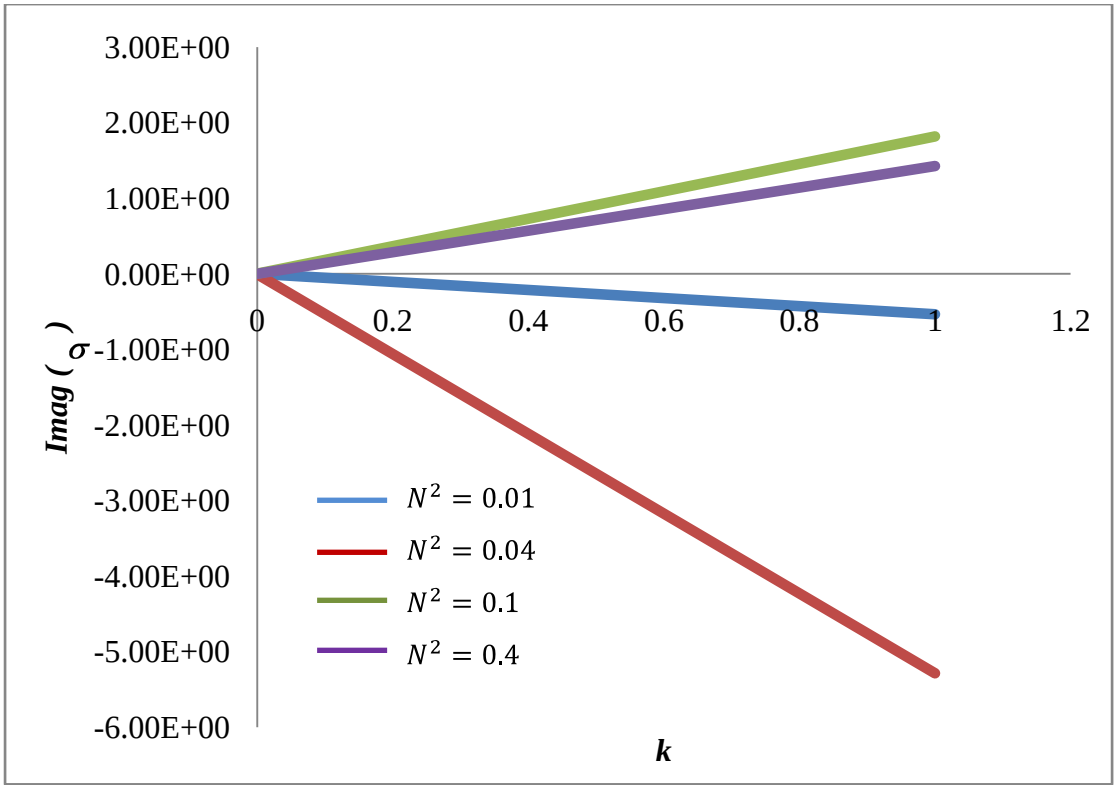

Figure 6.16: Growth rate as a function of wave number for various N^2

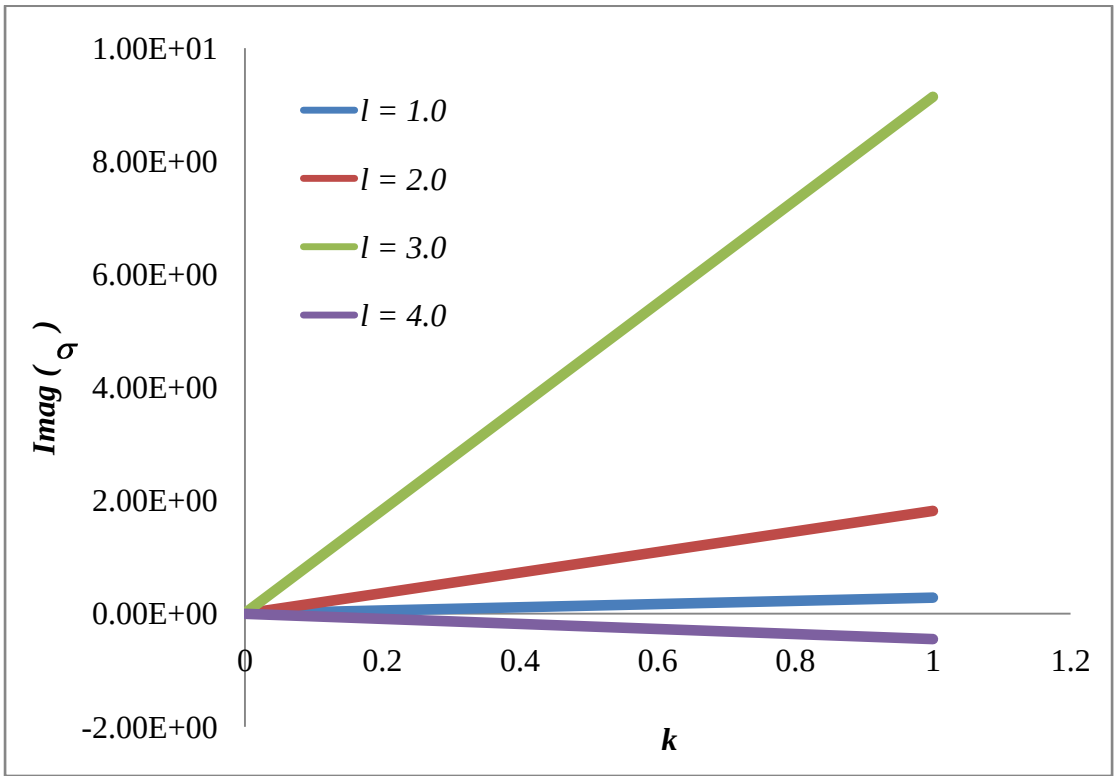

Figure 6.17: Growth rate as a function of wave number for various l

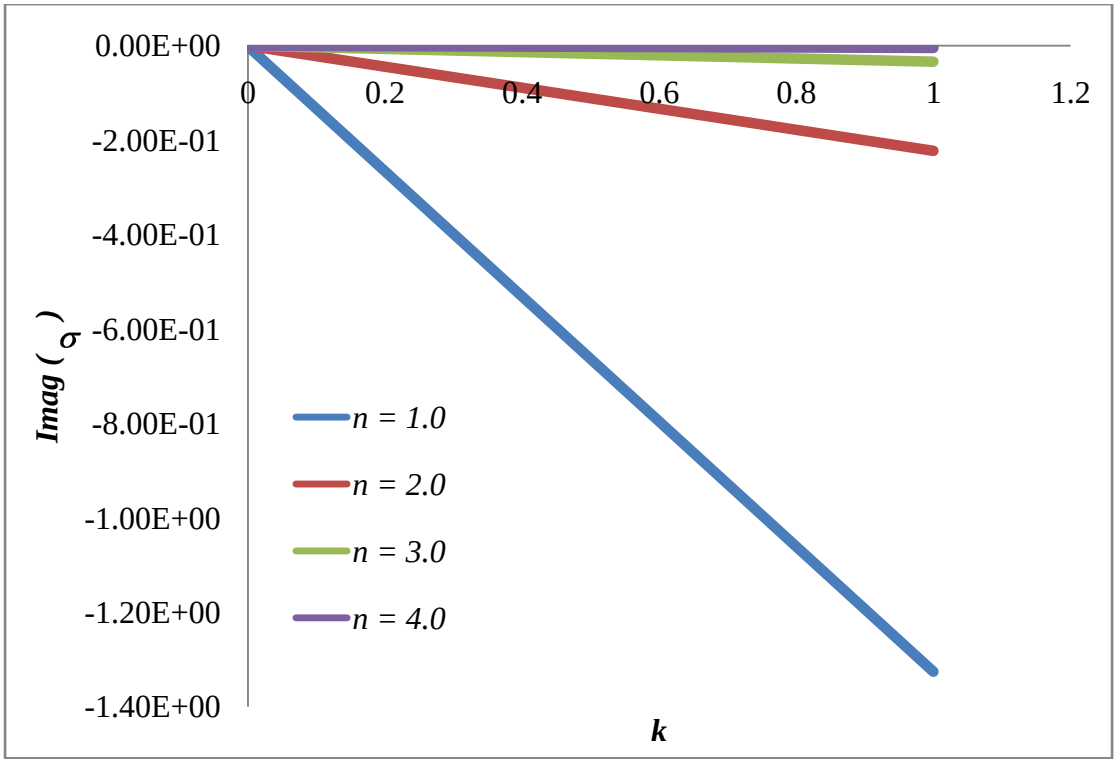

Figure 6.18: Growth rate as a function of wave number for various n

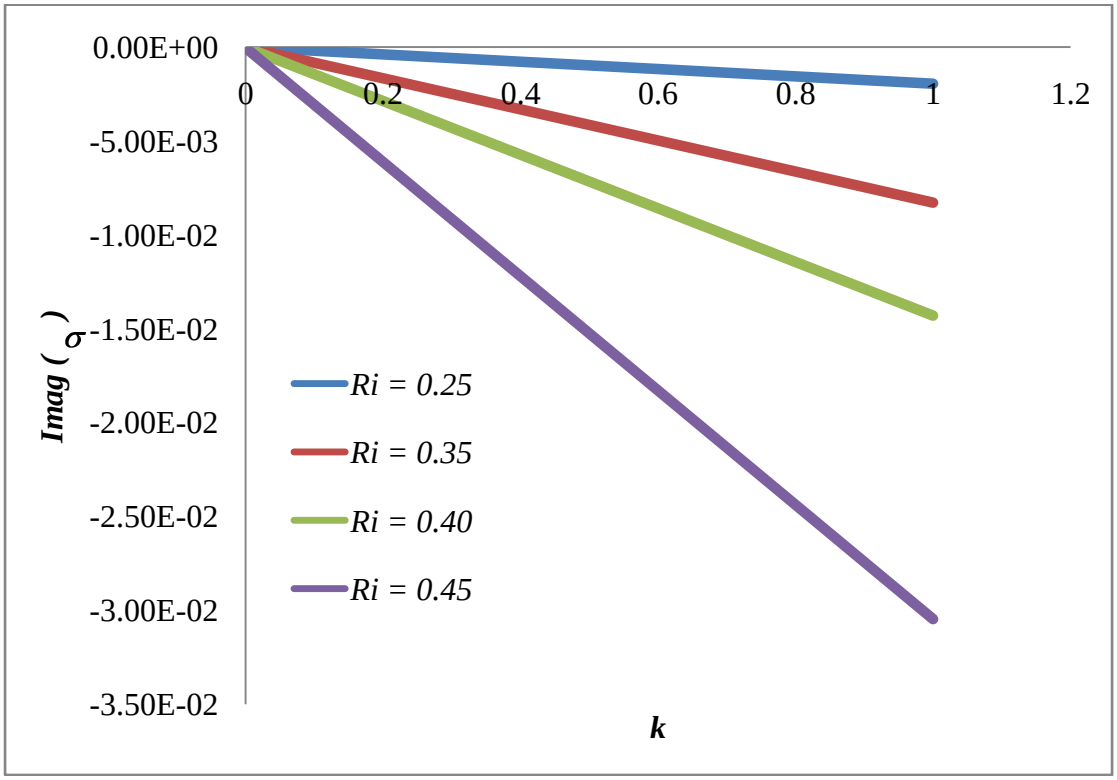

Figure 6.19: Growth rate as a function of wave number for various Ri

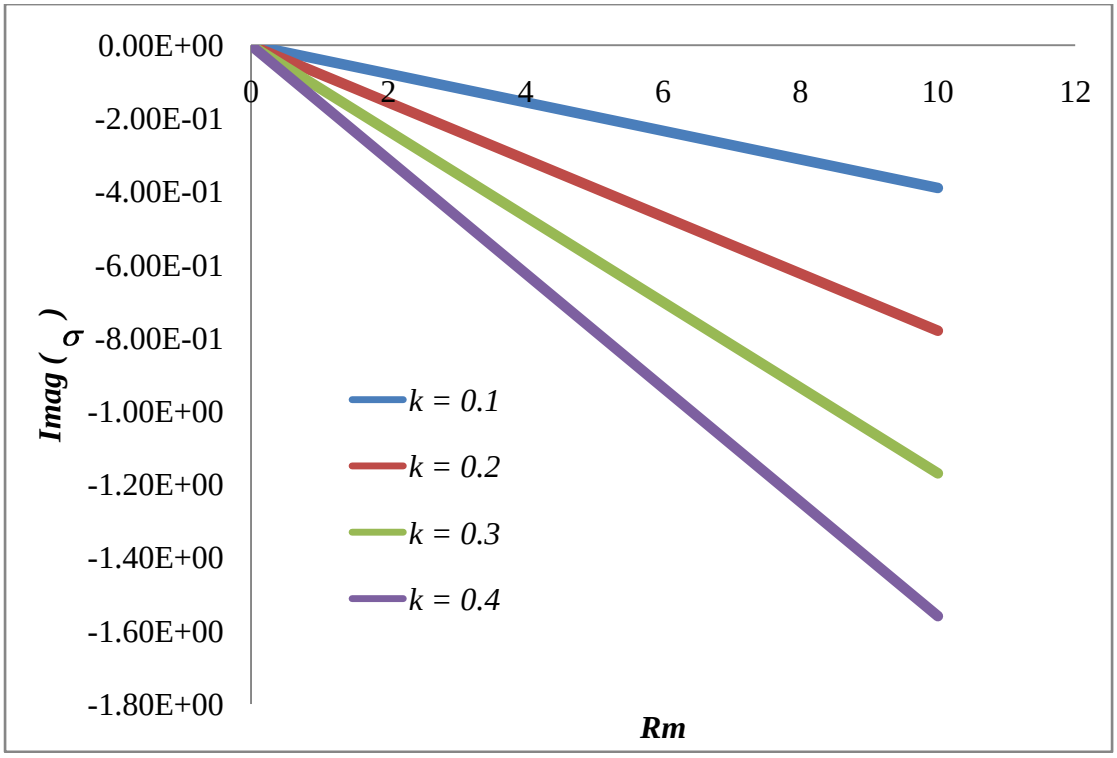

Figure 6.20: Growth rate as a function of Magnetic Reynolds number for various k

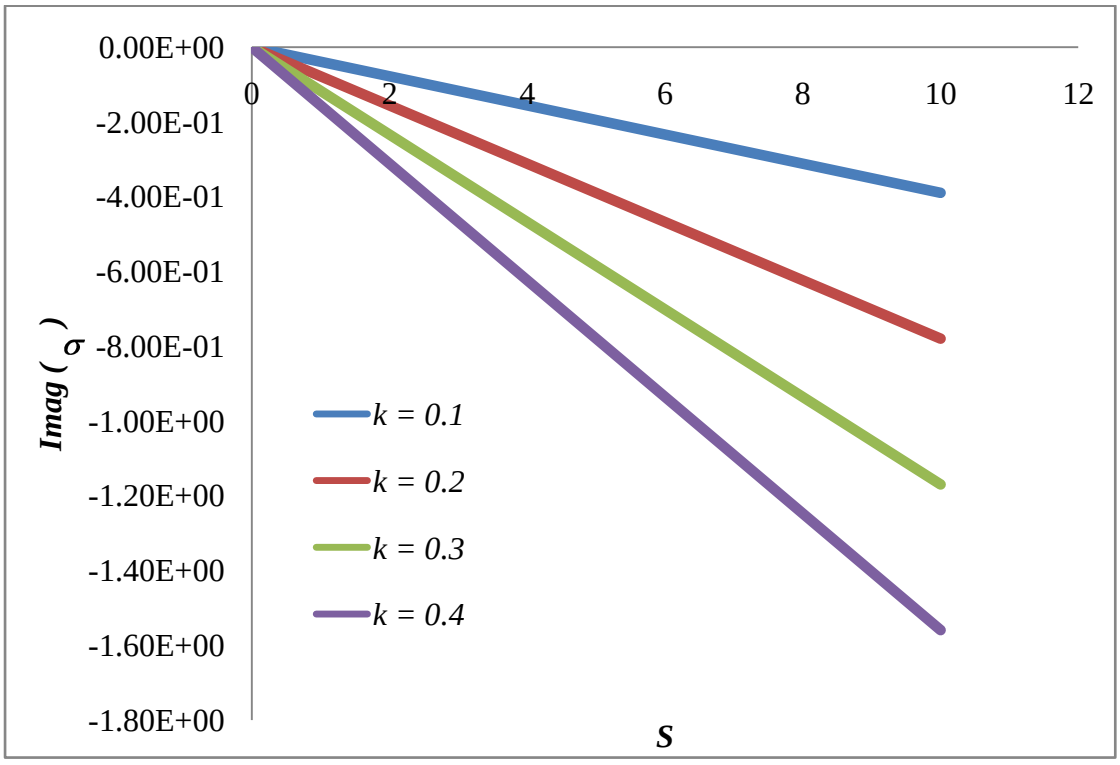

Figure 6.21: Growth rate as a function of Magnetic pressure number for various k

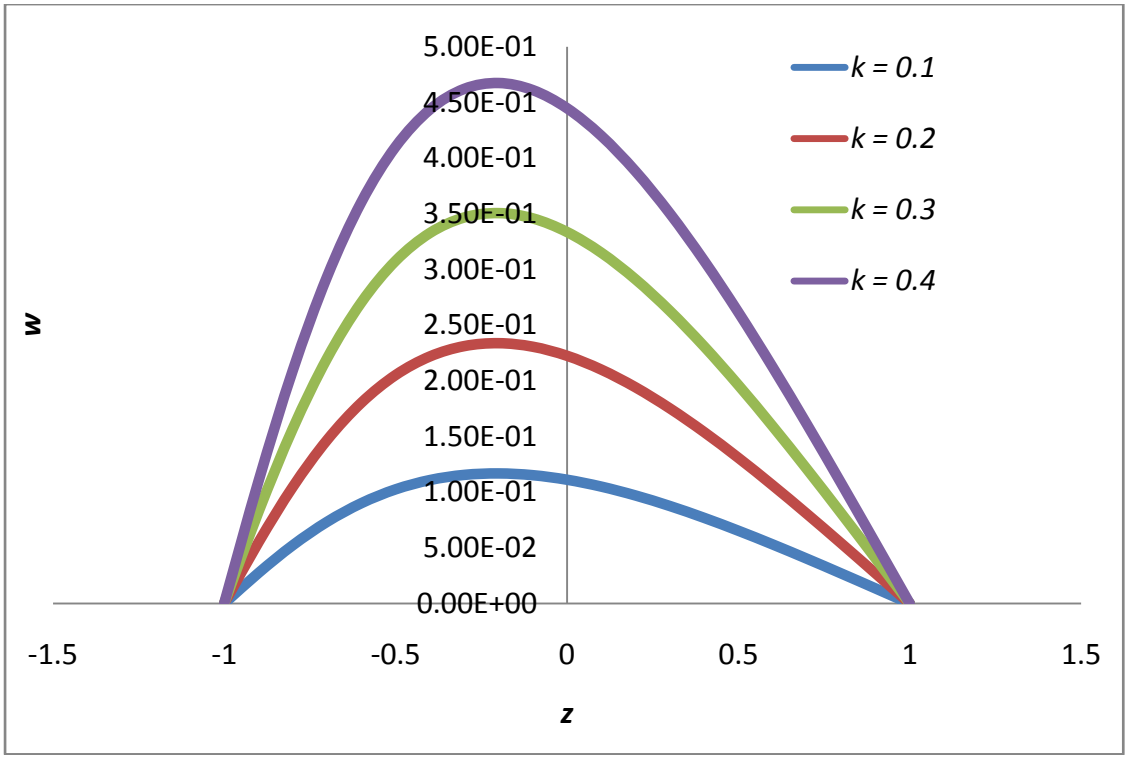

Figure 6.22: Effect of small wave number (k) on velocity profile ($\lambda > 0$)

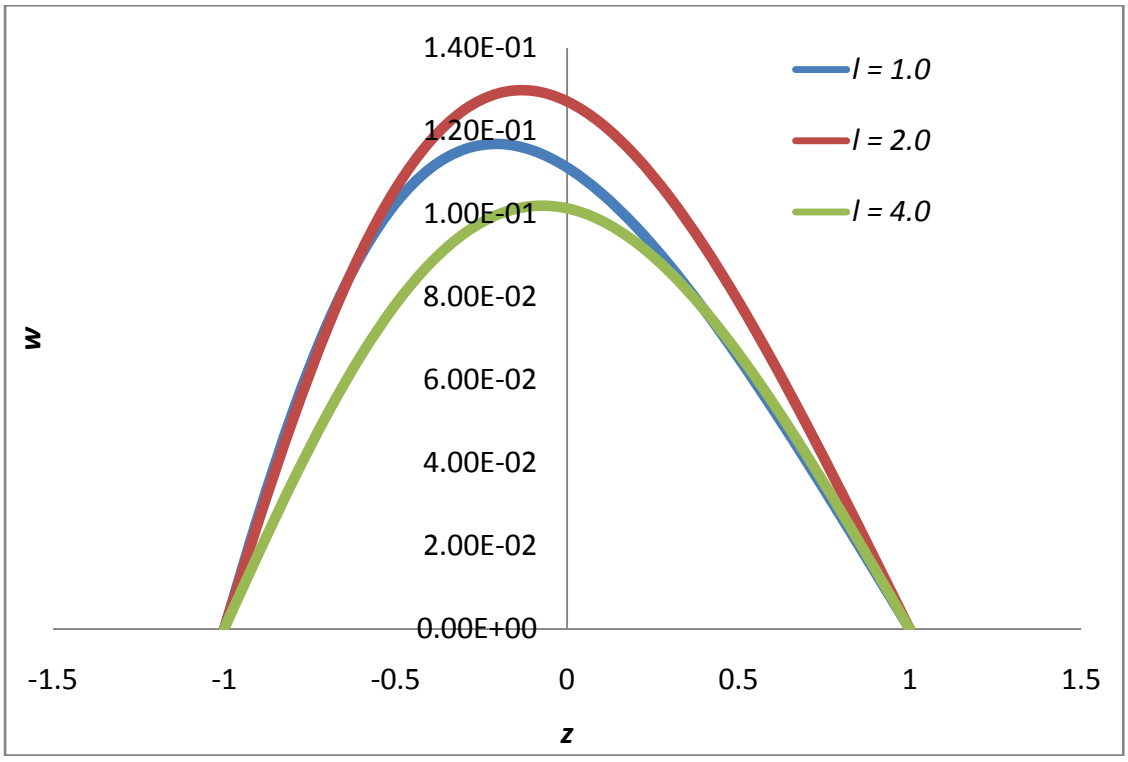

Figure 6.23: Effect of transverse wave number (l) on velocity profile ($\lambda > 0$)

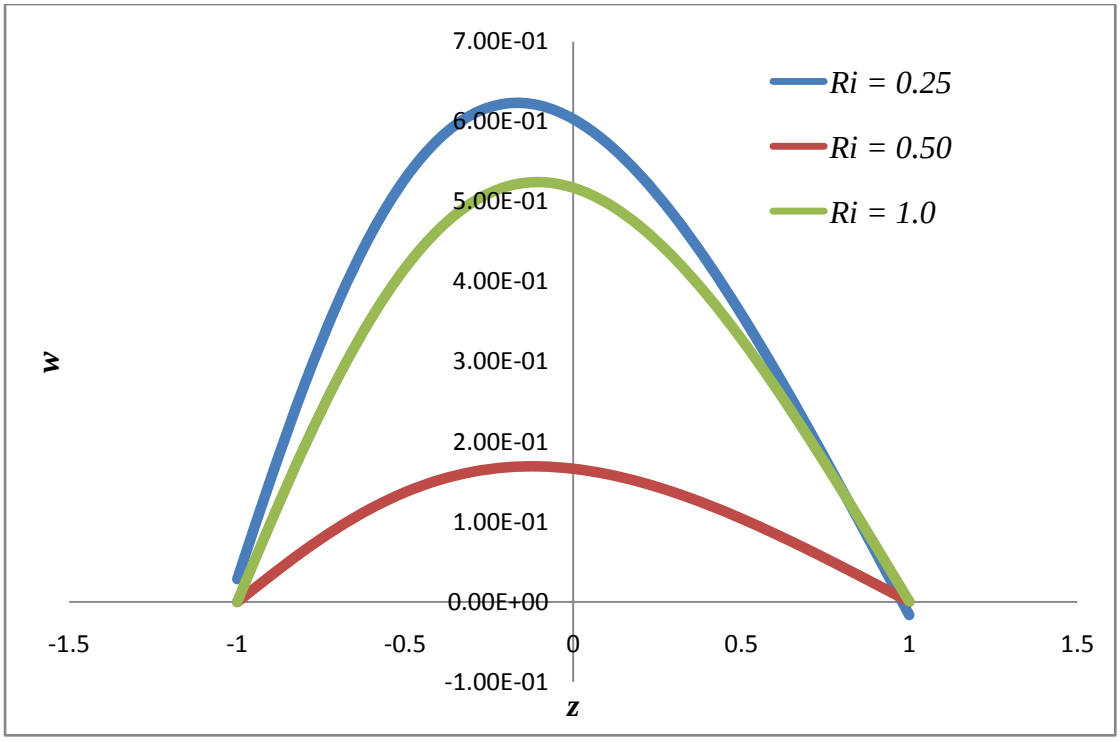

Figure 6.24: Effect of Richardson number (Ri) on velocity profile ($\lambda < 0$)

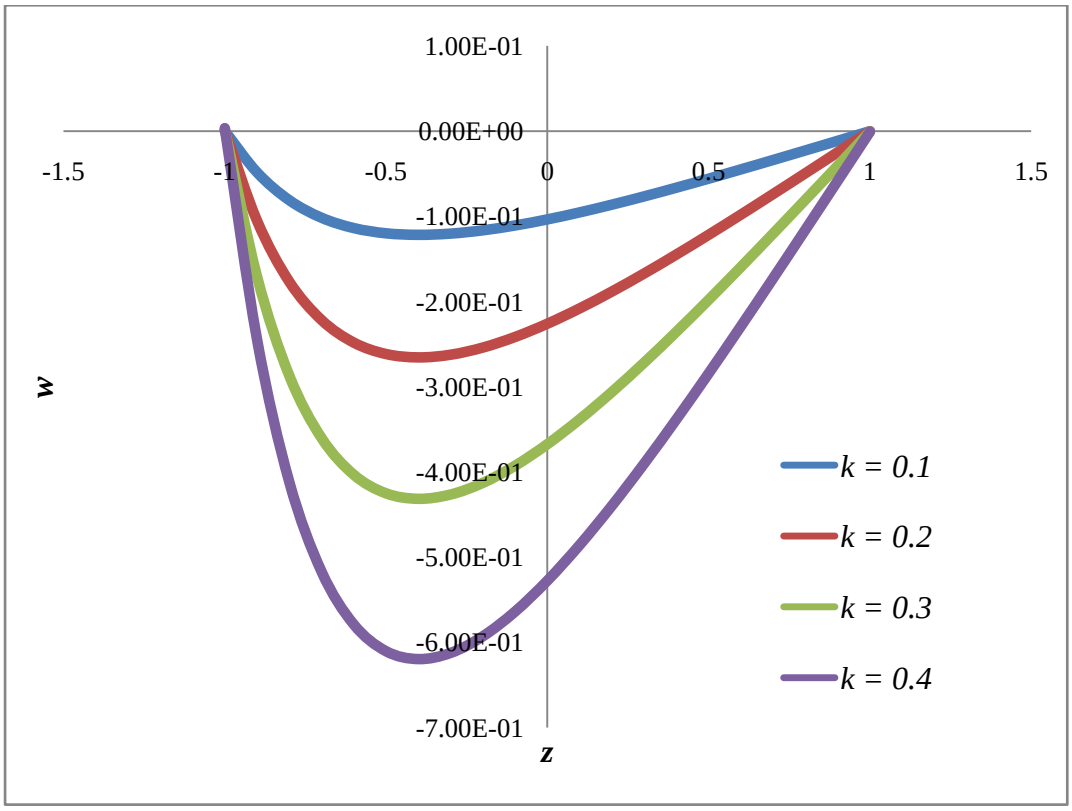

Figure 6.25:Effect of small wave number (k) on velocity profile ($\lambda < 0$)